

Boson stars: Chemical potential and quark condensates

Jitesh R. Bhatt* and V. Sreekanth†

Physical Research Laboratory, Ahmedabad 380009, India

We study equilibrium solutions of a boson star in mean field approximation using a general relativistic framework. Dynamics of the constituent matter in such a star is described by a scalar field. The statistical aspect of the matter equilibrium is investigated by incorporating the effect of finite chemical potential in equation of state. We analyze the two possible situations where the scalar field is either a composite one -suitable for describing diquark-condensates or a fundamental. We derive a generalized set of Tolman-Oppenheimer-Volkov (TOV) equations to incorporate the metric dependence of chemical potential in general relativity. It is demonstrated that the introduction of finite chemical potential can lead to a new class of the solutions where the maximum mass and radius of a star change in a significant way. In general the density profile has node like structures due to introduction of finite chemical potentials. It is shown that these nodes can be avoided by applying constraints on the values of the central pressure and central chemical potential. This in turn can reduce the parameter space available for the stable solutions. We also discuss the case when the boson star is made of diquark condensates. It is shown that when the self-interaction of the condensate is negligible, the typical energy density of the star is too high to have a boson star of diquark condensates. Our results indicate, even after the effect of self-interaction is incorporated, the stable equilibrium can occur only in a low-density and high-pressure regime.

PACS numbers:

I. INTRODUCTION

The boson stars are very fascinating objects as their self-gravity is not balanced by the degeneracy pressure like the other compact stars such as a white dwarf or a neutron star, but the Heisenberg uncertainty play a crucial role in their stability (see Ref. [1] for a recent review). Wheeler was first to consider the boson star in 1955 when he studied the stable equilibrium generated by the self-gravitating photons called *geons* [2]. Later Kaup analyzed a new class of boson stars as a self-consistent solutions of Einstein-Klein-Gordon equations in Ref. [3]. Since then the most of the boson star studies focus on the the stars made of self-gravitating scalar-field [1, 4]. This is because there are good reasons to believe that there exists a some fundamental scalar field in nature even though no experiment has detected it so far. The solutions found by Kaup in Ref. [3] were shown to describe the ground state of boson stars without using any perfect-fluid approximation or some approximation to equation of state by Ruffini and Bonazzola [5]. However in this work the self-interaction of the scalar-field was ignored. Subsequently it was shown by Colpi et. al. [6] that inclusion of even a very small interaction term can significantly alter the solutions obtained in Refs. [3, 5]. It turns out that the inclusion of a small interaction term in the scalar field Lagrangian give rise to an additional pressure that would help the Heisenberg uncertainty to counter

the self-gravity. This results in a boson star with much larger mass than ones reported in Refs. [3, 5]. Also the issues of dynamical stability of boson stars have been rigorously analyzed by applying perturbative methods [7]. Also are studies that show that there can be a boson star in the galactic center [8]. At present a very intriguing situation persists in the field: on the one hand there is no observational evidence which can indicate that a boson star exists, on the other hand their existence seem to be a reasonable consequence of well-tested physical theories like general relativity and Klein-Gordon equations. This should be a good enough reason, in our opinion, to further investigate the properties of boson stars.

Boson stars with a repulsive self-interaction mediated by vector mesons within the effective theory framework were studied only recently [9]. It is found that mass-radius curves satisfy the scaling properties for arbitrary boson masses and interaction strengths. There exist another novel possibility of having a boson star with a composite scalar field. Such a composite scalar field can possibly arise when the superconducting colour quark matter undergo a transition from the BCS phase to Bose-Einstein condensation phase via a so called BCS-BEC transition [10, 11]. It should be noted that BCS regime of the colour superconducting phase is well studied using the techniques of perturbative QCD. But in BCS-BEC crossover can occur in low density and low temperature regime, where the coupling constant is large and the perturbative techniques are not available. One may use the methods of effective theory to describe the matter in the strongly coupled regime. In this picture, instead of a repulsive vector-meson exchange one may have repulsive self-interaction of the scalar field describing the (diquark)

*Electronic address: jeet@prl.res.in

†Electronic address: skv@prl.res.in

condensates [10]. A diquark-BEC phase may occur at low density regime somewhere between colour neutral nuclear matter and the free quark phases. This requires an additional constraint namely - the size of the condensates or the coherent length ξ should not be larger than the inter-particle spacing i.e. $n^{-1/3}$, where n is the number density.

In this work we analyze the equilibrium solutions of a boson star in a low temperature finite chemical potential regime. As far as we know boson stars with a finite chemical potential are not properly considered in the literature. Majority of study do not focus on the statistical aspect of the self-gravitating boson gas but they rather appeal to find a specific equilibrium (quantum) solution of the Einstein-Klein-Gordon system. In the context of quark star we would like to mention that possibility of diquark star has already been considered in the literature [12]. However the effect of Bose-Einstein condensation was not considered in this work. This effect can be significant in a low temperature finite chemical potential regime [10]. Moreover, in general relativity temperature and chemical potential are local functions of space and time and therefore they depend upon the metric. The metric dependence of these quantities can be specified by using the well-known Tolman conditions for a thermal equilibrium in the gravitational field [13, 14]. Again this aspect was not considered in the literature on boson or diquark stars. In this work we derive a generalized set of Tolman-Oppenheimer-Volkov equations by incorporating the effect of metric dependence of chemical potential. This has resulted in an additional differential equation describing the space-time evolution of the chemical potential coupled with the TOV [15] equations.

In a very high density system such as a boson star, the introduction of finite chemical potential can rise a question. However in the standard model, for example, quark numbers are conserved and one can introduce chemical potential for them. In addition for a BCS-BEC crossover kind of transitions chemical potential play a very important role [10]. Chemical potentials are known to alter the global minimum of a scalar-field. In this work have demonstrated that when the scalar field mass m is comparable to the chemical potential μ , the mass-radius relations and the maximum mass of the star are significantly changed.

In what follows we first derive the generalized set of TOV equations and study their numerical solutions by providing the equation of state as an input. The equation of state is derived in the mean-field approximation. We use for the parameter values of the diquark phase in a manner consistent with that given in Ref. [10].

II. FORMALISM

Lagrangian density for the scalar-field can be written as

$$\mathcal{L} = -\sqrt{|g|} \mathcal{L}_\Phi$$

with

$$\begin{aligned} \mathcal{L}_\Phi = & - [g^{\mu\nu} \partial_\mu \Phi^\dagger \partial_\nu \Phi + i\mu g^{00} \delta_0^\alpha (\Phi^\dagger \partial_0 \Phi - \Phi \partial_0 \Phi^\dagger)] \\ & - U(|\Phi|^2) \end{aligned} \quad (1)$$

where, the potential $U(|\Phi|^2)$ is defined as

$$U(|\Phi|^2) = (m^2 + g^{00} \mu^2) |\Phi|^2 + g |\Phi|^4. \quad (2)$$

The energy-momentum tensor $T_{\mu\nu}(\Phi)$ written from this as follows:

$$\begin{aligned} T_{\mu\nu} = & [\partial_\mu \Phi^\dagger \partial_\nu \Phi + \partial_\mu \Phi \partial_\nu \Phi^\dagger] \\ & + i\mu g^{00} g_{0\mu} [\Phi^\dagger \partial_\nu \Phi - \Phi \partial_\nu \Phi^\dagger] + g_{\mu\nu} \mathcal{L}_\Phi \end{aligned} \quad (3)$$

The equations of motion of the scalar field is given by

$$\square + 2i\mu g^{00} \partial_0 + \frac{dU}{d|\Phi|^2} = 0 \quad (4)$$

where

$$\square := -\frac{1}{\sqrt{|g|}} \partial_\mu (\sqrt{|g|} g^{\alpha\mu} \partial_\alpha) \quad (5)$$

We are considering the 'standard' form of a spherically symmetric and static space-time metric [16] given by

$$ds^2 = -B(r)dt^2 + A(r)dr^2 + r^2(d\theta^2 + \sin^2 \theta d\phi^2), \quad (6)$$

where, we have used the units in which speed of light $c = 1$. Next to study the equilibrium configuration, we use the stationarity *ansatz* $\Phi(r, t) = \phi(r)e^{-i\omega t}$. Now the energy density ρ and pressure p can be obtained from the energy-momentum tensor:

$$\rho = \frac{T_{tt}}{B} = \frac{(\omega^2 - \mu^2)}{B} |\Phi|^2 + m^2 |\Phi|^2 + g |\Phi|^4 \quad (7)$$

and

$$p = \frac{T_{rr}}{A} = \frac{(\omega + \mu)^2}{B} |\Phi|^2 - (m^2 |\Phi|^2 + g |\Phi|^4). \quad (8)$$

And finally the equation of motion for the scalar field gives,

$$\frac{(\omega + \mu)^2}{B} = m^2 + 2g |\Phi|^2. \quad (9)$$

It must be noted here that while writing equations (7-9) we have dropped the spatial derivative terms of the

scalar field. It can be shown that $\frac{d\phi}{dr}$ is of the order of Λ^{-1} . Here $\Lambda = \frac{gM_{plank}^2}{2\pi m^2}$ is an extremely large number ($> 10^{30}$) for the parameter regime of the interest. This is equivalent to the mean field approximation ($\partial_r \Phi = 0$). Under this condition one can use the TOV equation to describe a self-gravitating bose star [6].

Using equations (7-9) one can rewrite p and ρ

$$p = g |\Phi|^4 \quad (10)$$

$$\rho = \rho_0 \left[4 \left(1 - \tilde{\mu} \sqrt{1 + \sqrt{\tilde{p}}} \right) \sqrt{\tilde{p}} + 3\tilde{p} \right] \quad (11)$$

where, $\rho_0 = \frac{m^4}{4g}$, $\tilde{\mu} = \frac{\mu/m}{\sqrt{B}}$ and $\tilde{p} = p/\rho_0$ is the dimensionless pressure. Equation (11) is equivalent to the EOS considered in Refs. [1, 6, 17] in the limit $\mu = 0$. In the limit of vanishing self-interaction i.e $g \rightarrow 0$, we have $p = 0$. In this limit self-gravity of the star will be balanced by the effect of Heisenberg uncertainty principle only [3, 18]. For high values of the \tilde{p} the last term in parenthesis of equation (11) dominates over the other terms, the EOS approach the relativistic limit i.e. $\tilde{\rho} = 3\tilde{p}$.

The form of functions $A(r)$ and $B(r)$ in equation (6) can be determined from the Einstein's field equations,

$$R_{\mu\nu} - \frac{1}{2}g_{\mu\nu}R = -8\pi GT_{\mu\nu}. \quad (12)$$

With the metric defined previously we get the relevant equations from (12) as,

$$\frac{A'}{rA^2} + \left(1 - \frac{1}{A}\right) \frac{1}{r^2} = 8\pi G \left(\frac{T_{tt}}{B}\right) \quad (13)$$

$$\frac{B'}{rAB} - \left(1 - \frac{1}{A}\right) \frac{1}{r^2} = 8\pi G \left(\frac{T_{rr}}{A}\right), \quad (14)$$

where ' denotes differentiation with respect to r . With $A(r) = (1 - 2GM(r)/r)^{-1}$, we get the stellar structure equations as,

$$\frac{B'}{B} = \frac{2G}{r^2} \frac{[M + 4\pi r^3 p]}{(1 - \frac{2GM}{r})}, \quad (15)$$

$$\frac{dM}{dr} = 4\pi r^2 \rho(r). \quad (16)$$

Hydrostatic equilibrium expressed as [16],

$$\frac{B'}{B} = -\frac{2p'}{p + \rho} \quad (17)$$

can be used to rewrite the equation (15) as

$$p' = -\frac{G}{r^2} \frac{[\rho + p] [M + 4\pi r^3 p]}{(1 - \frac{2GM}{r})} \quad (18)$$

The equations (16) and (18) are known as the TOV equations [15], which has to be solved together with the equations of state. But in our case ρ is a function of chemical potential μ , which in turn depends on the metric. Metric dependence of μ can be understood using equation (17) and thermodynamic Gibbs-Duhem relation,

$$d\frac{p}{T} = n d\frac{\mu}{T} - \rho d\frac{1}{T} \quad (19)$$

and can be written as [14],

$$\frac{B'}{B} = -\frac{2\mu'}{\mu}. \quad (20)$$

Finally the we get the desired relation with the help of equation (15) as,

$$\mu' = -\mu \frac{G}{r^2} \frac{[M + 4\pi r^3 p]}{(1 - \frac{2GM}{r})}. \quad (21)$$

So *generalized stellar structure equations in presence of chemical potential* are given by equations (16),(18) and (21). These equations are to be solved simultaneously with equation(11), to find out the properties of stellar configurations.

III. RESULTS AND DISCUSSION

Before solving stellar structure equations numerically let us consider the following qualitative arguments. First consider the case when there is no self-interaction term and also no chemical-potential i.e. $g = 0$ and $\mu = 0$. In this case the critical mass and radius of the star given $R \sim \frac{1}{m}$ and $M = M_{plank}^2/m$ [3]. Next, if the boson mass is around 100GeV , the corresponding critical mass of the star would be $M = 10^{17} M_{plank} \sim 10^9 \text{kg} \sim 10^{-21} M_N$ and its radius $R \sim 10^{-22} R_N$ where, M_N and R_N are mass and radius of a neutron star. Consequently, the density of such a boson star would be 10^{45} times that of neutron star. Thus for a diquark-condensate with mass $(0.5 - 1)\text{GeV}$ [10], the density of the corresponding star would be 10^{41} times of that of a neutron star. This is an extremely large value of the matter density for a diquark star to exist. However, things can change if the self-interaction term is nonzero. It is known that for the case $g \neq 0$ (and $\mu = 0$), the scalar-field $|\Phi|$ scales as M_{Plank}/Λ if $\Lambda = \frac{gM_{plank}^2}{2\pi m^2} \gg 1$ [6]. This condition is to satisfy even for a very small values of g . Comparing the quadratic and quartic terms in the potential U , we get $\frac{g|\Phi|^4}{m^2} \sim \Lambda \frac{|\Phi|^2}{M_{plank}^2} \sim O(1)$. The energy density ρ will be about $m^2 M_{plank}^2/\Lambda$. Thus the energy density would corresponds to that of a non-interacting boson if mass is rescaled as $m \rightarrow m\sqrt{\frac{1}{\Lambda}}$. From this the maximum mass

can be found [3, 19] to be

$$M_0 \approx \frac{2}{\pi} \sqrt{\Lambda} \frac{M_{planck}^2}{m} \quad (22)$$

This also matches with the estimate critical mass obtained numerically in Ref. [6]. In our case, in the flat space, the classical potential has non-trivial minimum at $|\Phi|^2 = \frac{\mu^2 - m^2}{2g}$. We have assumed that $m^2 > 0$ and for $\mu^2 > m^2$ we have condensation. In this case the mass scaling will be different and it is given by $m \rightarrow m/\sqrt{\Lambda} \left(\frac{\mu^2}{B} - 1 \right)$ and the maximum mass may be given by $\sqrt{\Lambda} \frac{M_{planck}^2}{m} \left(\frac{\mu^2}{B} - 1 \right)$. This suggest that the maximum mass should decrease if the chemical potential is decreasing. Since the chemical potential term here depend on space-time the above is only a rough estimate of the maximum mass. It also must be noted that the above arguments are not valid if $\frac{(\mu/m)^2}{B} < 1$.

The validity condition $\xi < n^{-1/3}$ for the condensate description. $\xi (= \frac{1}{\Delta})$ can be found from the gap equation [20]

$$\Delta = 2\mu \exp\left(-\frac{3\pi^2}{\sqrt{2}g}\right), \quad (23)$$

for $\mu \approx 400 - 500 MeV$ and the corresponding running coupling constant 3.56. However, at this juncture the above equation should not be taken too seriously as it is based upon the arguments of the perturbation theory. The BCS-BEC transition is supposed to take place in the high coupling regime. The quark-condensation condition in the flat-space is $(\mu/m)^2 > 1$ [10]. However, in the case of a boson star it needs to be locally satisfied.

Next, we write the generalized TOV equations in a dimensionless form. We have already introduced the dimensionless variables for the pressure \tilde{p} , density $\tilde{\rho}$ and chemical potential $\tilde{\mu}$. We calculate the mass M in the dimensionless unit $\tilde{M} = M/M_o$ where M_o is the solar mass. Radius of the star (R) is also computed in terms of $\tilde{R} = R/R_o$, with $R_o = GM_o = 1.47 km$. Radius of the star can be defined as the distance from the center where ρ becomes zero. We solve equations (16, 18, 21) by specifying various values of the central pressure p_c and the chemical potential μ_c , while M at the center is considered to be zero.

From the form of equation (11) it is clear that, the energy density could be negative if the values p_c and μ_c are chosen arbitrarily. Therefore it is required to constrain their values by imposing the condition $\tilde{\rho} > 0$.

$\tilde{\rho} > 0$ condition and two branches of solutions :

The condition (on the initial conditions) implies that there are following two branches of the solutions:

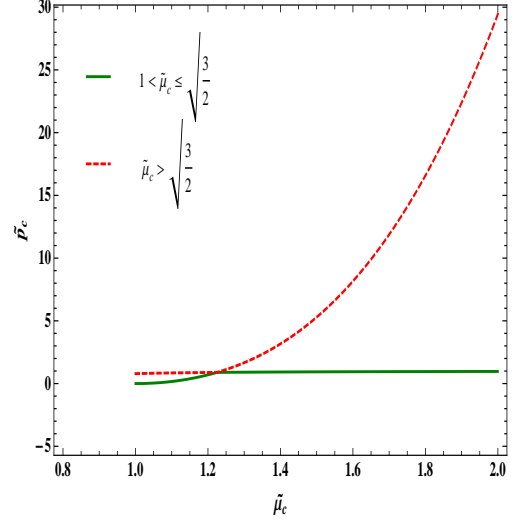


FIG. 1: The graph shows the solutions for initial conditions of pressure \tilde{p}_c and chemical potential $\tilde{\mu}_c$ for $\tilde{p}_c \geq 0$.

$$\tilde{p} \geq \frac{16}{81} (9 - 15\tilde{\mu}^2 + 8\tilde{\mu}^4) \quad (24)$$

$$- \frac{32}{81} \sqrt{-27\tilde{\mu}^2 + 72\tilde{\mu}^4 - 60\tilde{\mu}^6 + 16\tilde{\mu}^8}; \quad (1 < \tilde{\mu} \leq \sqrt{\frac{3}{2}})$$

$$\tilde{p} \geq \frac{16}{81} (9 - 15\tilde{\mu}^2 + 8\tilde{\mu}^4) \quad (25)$$

$$+ \frac{32}{81} \sqrt{-27\tilde{\mu}^2 + 72\tilde{\mu}^4 - 60\tilde{\mu}^6 + 16\tilde{\mu}^8}; \quad (\tilde{\mu} > \sqrt{\frac{3}{2}})$$

The solid curve in figure (1) represents the first branch given by equation (25), which is valid the values of chemical potential defined in the range $1 < \tilde{\mu} \leq \sqrt{\frac{3}{2}}$. The curve with the dotted line represents the branch given by equation (26). From figure (1) it is clear that solutions of the equation (25) is valid even in the region $1 < \tilde{\mu} \leq \sqrt{\frac{3}{2}}$.

Figure (2) shows the density profile as function of \tilde{r} for various values of the central pressure and the chemical potential $\tilde{\mu} = 1.5$. The solution indicates the nodes in the profiles. However, this is a unphysical behavior and it can be avoided by imposing the no-node condition on ρ .

No-Node condition : We need to make sure that $\tilde{\rho}'(r = 0) < 0$ inside the star. Analytically this condition can be represented as,

$$\left(2 + 3\sqrt{\tilde{p}(0)}\right) \left(\sqrt{1 + \sqrt{\tilde{p}(0)}} - \tilde{\mu}(0)\right) \tilde{p}'(0) - 4 \left(1 + \sqrt{\tilde{p}(0)}\right) \tilde{p}(0) \tilde{\mu}'(0) < 0 \quad (26)$$

The upper most curve in figure (2) is plotted by incorporating the no-node condition on the initial values

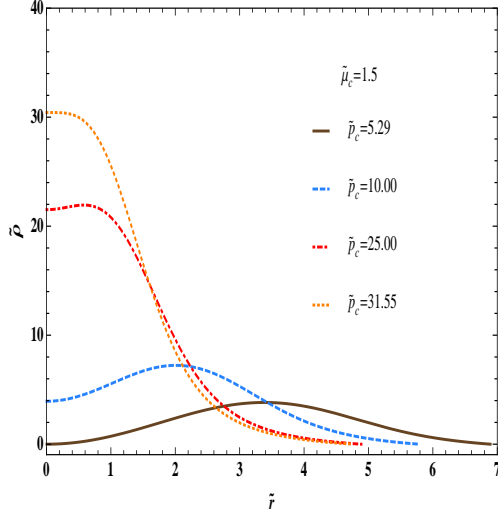


FIG. 2: For a given chemical potential the density profile can have nodes. The upper most curve is obtained by imposing the no-node condition.

of pressure and chemical potential. Thus the implementation of the no-node condition shows that for a given chemical potential there exist a lower bound on the central pressure. If one specify the central pressure below this bound then the nodes develops in the density profiles. Our numerical study indicates that if the initial values of the pressure and chemical potential are chosen just above the two branches of ' $\tilde{\rho} > 0$ condition' as shown in figure (1), the density profile develops the nodes. One can avoid the nodes for higher values of the central pressure p_c , but this will also increase the central density as implied by equation (11). It should be noted that the nodes in our analysis arise solely due to the introduction of the chemical potential and therefore their origin is different than the nodes in the wave functions reported in earlier literature of boson-star (for example [6]).

Figure (3) shows graph of the star-mass as a function of the central pressure for different values of the chemical potential. The lower most curve represents the case of zero chemical-potential. The mass is increasing with increasing the central pressure (density) and it reaches a plateau. This behavior is in agreement with the earlier work. Also the value of maximum-mass is in agreement with Ref. [6]. The introduction of a finite chemical-potential increases the overall value of the maximum-mass and the plateau. This figure shows that when the values of μ_c , increases, the maximum-mass values occurs at higher values of p_c . The lower values of p_c in this case ($\mu_c > 1$) are ruled out due to the no-node condition. If this condition is violated then the maximum-mass configurations would occur at much lower p_c . And in this case the maximum-mass would be much higher than the $\mu_c = 1$ case. Thus the consistent solutions with finite

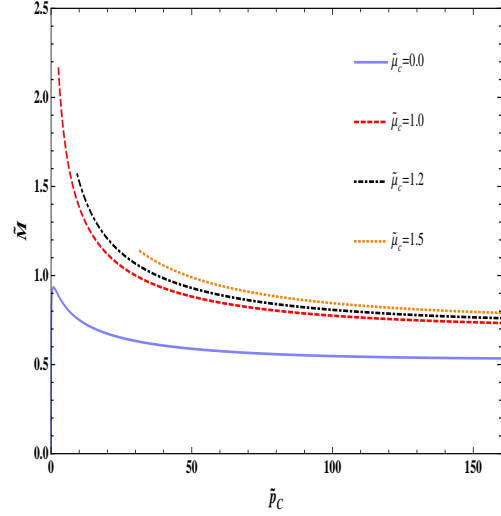


FIG. 3: Maximum Mass of the star versus initial pressure for different values of μ_c is plotted. The peak of the graph in each case denotes the highest maximum mass configuration.

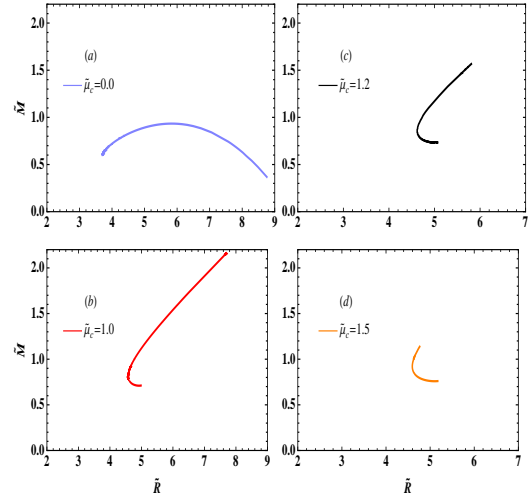


FIG. 4: Maximum Mass of the star versus Radius for different values of μ_c is plotted. The peak of the graph in each case denotes the highest maximum mass configuration.

chemical-potential requires to have higher values of the central-pressure in comparison with the $\mu_c = 0$ case.

In figure (4) we have plotted mass of the star versus radius for different values of the chemical-potential. The radius is determined by the value of radial coordinate $r (= R)$, where the density vanishes. The metric-dependence of the chemical-potential gives a new class of solutions. Figure (4a) shows the case of zero central chemical-potential, in this case there is no variation in the chemical-potential as implied by equation (21). In

this case, the maximum mass value occurs at the peak of the curve and its value matches well with the known result [6]. All the points on the left-hand side of the peak are unstable, as they have higher gravitational potential energy than the points on the right-hand side. Figure (4b) represents $\mu_c = 1$ case, one can see that the value of maximum-mass has increased as compared to $\mu_c = 0$ case and more strikingly the value of the maximum-mass does not occur on the peak of the curve. The spiral like structure in the lower part of the curve represents two branches of then solution. In this region for any given R there exist two points with the same mass. The points on the lower-arm of the spiral have minimum energy, while points on the upper-arm may be unstable. Figure (4c) shows the case with $\mu_c = 1.2$. Again the maximum-mass does not occur on the peak of the curve and its value is smaller than $\mu_c = 1$ case. Radius of the star at the maximum-mass point is much smaller than the case shown in figure (4b) and thus the density of the star is higher than $\mu_c = 1$ case. Figure (4d) shows that for $\mu_c = 1.5$, the maximum-mass is smaller than $\mu_c = 1.2$ case and it occurs at a smaller radius. In this case the maximum-mass point lie in the unstable region. The lower-arm of the spiral represents the stable branch of the solution. The maximum-mass point in the stable branch is comparable to the case shown in figure (4a). This points occurs when $(\frac{d\tilde{M}}{dR})^{-1} = 0$ is satisfied. It should be noted that the qualitative arguments for maximum-mass of a star, given below equation (22), may not be applicable for the cases shown in figure (4b-4d). As these arguments do not account for the variation in the chemical-potential and no-node condition imposed on the ρ .

Figures (5-6) show pressure and density as functions of \tilde{r} for the case when the central-pressure is kept fixed at $\tilde{p}_c = 35$ and vary $\tilde{\mu}_c$. Figure (5) indicates that the pressure decreases less slowly with r by increasing the value of chemical-potential. Thus the star radius may increase if the chemical-potential is increasing. The density vs. distance plot also shows the similar behavior. In this case the value of central-density $\tilde{\rho}_c$ is not fixed, but it decreases as the chemical-potential at center increases. This behavior is expected from the form of the EOS (11).

Figure (7) shows the typical variation in chemical-potential and the metric-function B with the radius. The metric-function approaches the unity at the boundary, while the value of the chemical-potential decreases from its central value with the radius. However, the value of $\tilde{\mu}$ remains non-zero at the boundary. The dynamics of the chemical-potential and B are complementary as can be anticipated from definition of $\tilde{\mu}$.

Let us consider the case when the scalar-field represents the diquark-condensates which may arise in a low-density and strong-coupling regime. The condition for

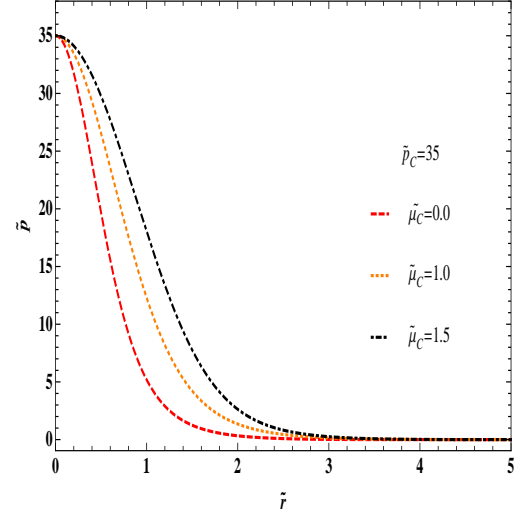


FIG. 5: The variation of the normalized pressure with the normalized radius for the different values of the central chemical-potential is shown here. The central pressure in all the cases is kept fixed.

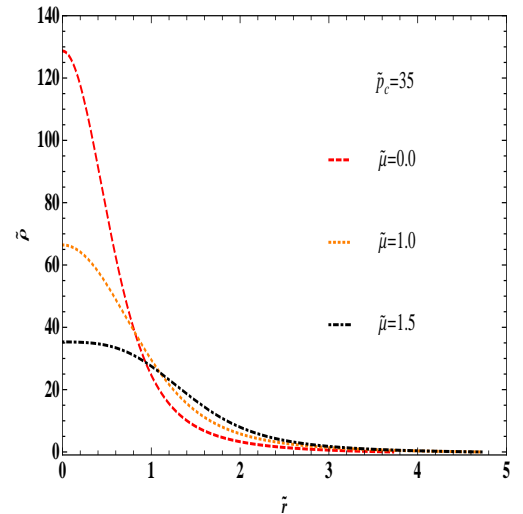


FIG. 6: The variation of the normalized density with normalized radius for the different values of the central-chemical potentials is shown here. The central pressure in all the cases is kept fixed.

the condensate formation is $(\mu/m)^2/B > 1$ or $\tilde{\mu}^2 > 1$. One can notice from figure (7) that this condition is violated somewhere inside the star. For the condition to be valid inside the entire region of the star one has to increase the value of $\tilde{\mu}_c$. From the discussion above, increasing $\tilde{\mu}_c$ would also requires to increase the central-pressure \tilde{p}_c . This may in turn increases the density as shown in figure (2). Clearly the energy density can not

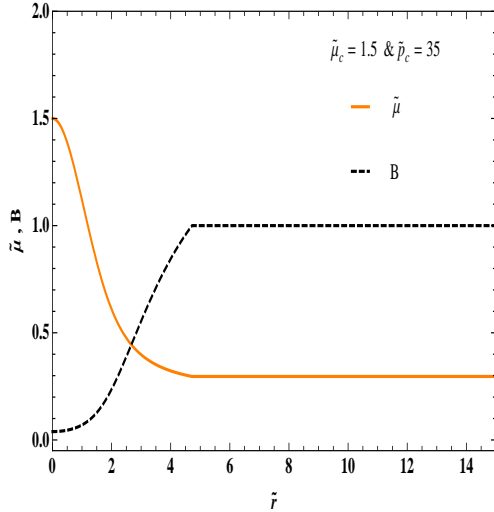


FIG. 7: The typical variation of the normalized chemical-potential and the metric-function B with the radius is shown for the given values of central pressure and chemical-potential.

increase to a very high values otherwise the condition of BEC formation may not be fulfilled. For example one may take the value of the chemical potential $\tilde{\mu}_c = 1.5$ which is consistent with [10]. According to the figure (2), the physical density profile should be around 30 times larger than the nuclear density which is not consistent with the BCS-BEC crossover assumption. Moreover, the mass-radius diagrams shown in figure (4) suggest that as $\tilde{\mu}$ increases the available parameter-space for the stable

configuration reduces significantly. We would like to add here that when one considers the case of fundamental scalar-field, the constraint of the low energy-density is not required. In this situation the boson-star equilibria are defined over a large range of the parameters.

IV. SUMMARY

Thus we have studied the properties of boson-stars in the mean-field approximation. We derived the generalized set of TOV equations to incorporate the effect of finite chemical potential. It is shown that chemical potential can introduce unphysical features like nodes in the equilibrium profile of the density which can be removed by imposing the no-node condition. No-node condition can put constraints on the physical values of the chemical potential and the pressure at the center of the star. The new class of solutions of the star that we have found show that available parameter space for the stable solutions gets greatly reduced by increasing the chemical potential. Further when our analysis when applied to the diquark condensate stars show that for a stable solution the density of the star needs to be too high for the diquark condensates to exist.

Acknowledgments

We would like to thank Dr. H. Mishra for the useful discussion.

-
- [1] F. E. Schunck and E. W. Mielke, astro-ph:0801.0307, F.E. Schunck and E. W. Mielke, Classical and Quantum Gravity **20**, 301,(2003).
 - [2] J. A. Wheeler, Phys. Rev.**97**, 511, (1955).
 - [3] D. J. Kaup, Phys. Rev.**172**, 1331(1968).
 - [4] P. Jester, Physics Reports **220**, 163(1992), T.D. Lee and Y. Pang, Phys. Rept. **221**, 251 (1992).
 - [5] R. Ruffini and Bonazzola, Phys.Rev.**187**, 1767(1969).
 - [6] M. Colpi, S.L. Shapiro and I. Wasserman, Phys. Rev. Lett.**57**, 2485 (1986).
 - [7] T.D. Lee and Y. Yang, Nucl. Phys. **B315**, 477 (1989), Ph. Jetzer Phys. Lett.**B243**, 36, (1990), M. Gleisser, Phys. Rev.**D39**, 1257(1989).
 - [8] D. G. Torres, S. Capozziello, and G. Lambiase, Phys. Rev. **D 62**, 104012 (2000).
 - [9] P. Agnihotri, J. Schaffner-Bielich and I.N. Mishustin, Phys. Rev. **D 79**, 084033 (2009); arXiv:0812.2770.
 - [10] A.H. Rezaeian and H. J. Pirner, Nucl. Phys. **A 779**, 197 (2006).
 - [11] M. Matsuzaki, Phys. Rev. **D62**, 017501 (2000), [hep-ph/9910541]; E. Babaev, Int. J. Mod. Phys. **A16**, 1175 (2002), [hep-th/9909052]; M. Kitazawa, T. Koide, T. Kunihiro and Y. Nemoto, Phys. Rev. **D65**, 091504(R) (2002), [nucl-th/0111022]; H. Abuki, T. Hatsuda and K. Itakura, Phys. Rev. **D65**, 074014 (2002), [hep-ph/0109013]; M. Kitazawa, T. Koide, T. Kunihiro and Y. Nemoto, Phys. Rev. **D70**, 056003 (2004), [hep-ph/0309026]; Y. Nishida and H. Abuki, Phys. Rev. **D72**, 096004 (2005), [hep-ph/0504083]; M. Kitazawa, T. Koide, T. Kunihiro and Y. Nemoto, Prog. Theor. Phys. **114**, 117 (2005); K. Nawa, E. Nakano and H. Yabu, Phys.Rev. **D74**, 034017 (2006); [hep-ph/0509029], H. Abuki, T. Hatsuda and K. Itakura, Nucl.Phys.**A791**, 117(2007); [hep-ph/0605081], L. He,

- P. Zhuang, Phys.Rev. **D75**, 096003 (2007), B. Chatterjee, A. Mishra, H. Mishra, Phys.Rev. **D79**, 014003 (2009)
- [12] D. Kastor and J. Traschen, Phys. Rev.**D44**, 3791(1991).
- [13] R.C. Tolman, *Relativity Thermodynamics and Cosmology*, (Clarendon, Oxford, 1934).
- [14] N. Bilic and R. D. Viollier, Gen. Rel. Grav.**31**, 1105 (1999).
- [15] J. R. Oppenheimer and G. M. Volkoff, Phys. Rev **55**, 374 (1939); R. C. Tolman, Phys. Rev **55**, 364 (1939).
- [16] S. Weinberg, *Gravitation and Cosmology*, John Wiley & Sons, Inc. (1972).
- [17] F. D. Ryan, Phys. Rev.**D55**, 6081 (1997).
- [18] E. H. Leib, Rev. Mod. Phys. **48**, 553 (1976).
- [19] J. Ho, S. Kim and B.H. Lee, arXiv:gr-qc/990240(1999), E. Mielke and F. Schunck; Proc. 8th M. Grossmann Meeting, T. Piran (ed.), World Scientific, Singapore (1998); [gr-qc/9801063], I.I. Tkachev, Sov. Astron. Lett **12**, 305(1986).
- [20] M. G. Alford, K. Rajagopal, T. Schaefer and A. Schmitt, Rev.Mod.Phys **80**, 1455 (2008).